Journal of Thermal Analysis and Calorimetry (2022) 147:711–726
https://doi.org/10.1007/s10973-020-10226-8

Numerical heat transfer analysis and development of a heat removal system for an unshaded parked car in sunny day: computational fluid dynamics study

Vishal Shankar Rath[1] · S. Senthilkumar[2] · Dewanshu Deep[2]

Received: 25 January 2020 / Accepted: 3 September 2020 / Published online: 15 September 2020
© Akadémiai Kiadó, Budapest, Hungary 2020

Abstract
Increase in air temperature inside a parked car cabin causes negative impacts such as low thermal comfort, health risk for the passengers/pets inside the cabin, increased fuel consumption due to higher air-conditioning requirements. The present project focuses on methods to reduce the cabin temperatures for a car parked in unshaded condition. CFD analyses along with experimental validation have been performed with the use of different proposed cabin temperature control methods such as use of electrochromic tint on windshield, use of inlet and outlet vents, lowering of windows and combinations of these. Commercial CFD package ANSYS Fluent has been utilized to develop a numerical model for car cabin temperature distribution assessment when a parked car is subjected to solar load at different locations inside the cabin such as dashboard, seats and boot. A solar surface to surface radiation model is used in conjunction with solar calculator to capture the solar radiation that included change in position of the sun. A 5:1 scale down model of car cabin has been used for experimental validation with the help of help of PT-100 resistance thermometers. Good reduction in cabin temperatures has been observed for all the proposed cooling methods with 14 °C reduction for the combined tint, vents and lowered windows case.

Keywords Car cabin · Solar load · Heat removal system · Tint · Vents · Numerical

Introduction

Regulation of the cabin temperature in automobiles is a major factor in determining the overall comfort of a passenger. The air-conditioning systems presently in use are not very efficient and add a significant load on the vehicle power source. The temperature inside the vehicle cabin will be higher than the outside environment temperature in parked conditions due to solar radiative effects. The increased air temperatures inside car cabins, especially when parked under intense solar radiation, poses several threats such as: health risk for the passengers and low thermal comfort, impact on the quality and durability of cabin materials like plastics, foams or artificial leather, rubber, synthetic fibre, etc., and increased fuel consumption. [1]

Booth et al. [2] have carried out a study on the circumstances of child fatalities due to children left in parked cars, known as Motor vehicle-related child hyperthermia fatalities (MVRCHF). Two hundred and thirty one fatalities in the USA were analysed in their study between 1999 and 2007. These are considered avoidable deaths which can be prevented through proper cooling methods and caution from users. Johnson [3] has conducted a study to determine the average amount of fuel used by a vehicle's air-conditioning system. He has carried out a detailed analysis of different USA states to observe the trends in fuel consumption due to thermal management needs. These studies emphasize on the need of effective thermal management systems for a vehicle in order to reduce the negative impacts of cabin heating. Reduction of the heat soaked by vehicles and improved or alternative cabin cooling systems can prove useful in the purpose.

Sen and Selokar [4] study the cabin cooling effectiveness and the cabin airflow patterns using CFD. They have

✉ S. Senthilkumar
s.senthilms@gmail.com

[1] Department of Automobile Engineering, Vel Tech Rangarajan Dr. Sagunthala R&D Institute of Science and Technology, Chennai, Tamil Nadu 600062, India

[2] Department of Aerospace Engineering, SRM Institute of Science and Technology, Kattankulathur, Kanchipuram, Chennai, Tamil Nadu 603203, India

accounted for solar heat loads on the car and cabin soaking for the heat sources. They have modelled the air flow patterns inside the cabin in presence of passengers and tried to identify the regions of low and high circulation. The load on the cooling system was monitored and compared through both steady state and transient simulations. Khatoon and Kim [5] have used Fluent to study three different ventilation systems with the effectiveness and efficiency of each along with the comfort of the passengers when the car is parked under direct sunlight. The modified Fanger's model was observed to give 20% improvement in thermal comfort of passengers. They have also attempted at predicting the most comfortable seating location for a child in the car under given conditions.

Jha et al. [6] have created a simplified model for predicting the cooling loads inside the cabin of a car parked in the sun. They have included from solar radiation load, load from electrical fittings and occupants, and air leakage; they have also included the effect of ground-reflected radiation and air mass. They have attempted to reduce the computational time and resource demand for complex 3-D simulations through their model and verified their results from wind tunnel tests for the same. They have found their model to be in acceptable range of the experimental results. On similar grounds Patil et al. [7] have developed a 1-D mathematical model for thermal assessment of an automobile cabin using Modelica language. They have carried out simulations for a car parked in the sun for 2 h with a solar radiation model along with changing sun position. They have validated their results with available 3-D simulation results and found very low deviations.

Several experiments have been carried out with actual cars placed in real-life conditions for monitoring cabin heat and its removal. Arya [8] studied cabin temperature control of a parked car through forced ventilation. Tseng et al. [9] have attempted to reduce the load on the car's cooling system, hence increase the range of an electric car. A 5:1 scale model was used and the effect of different methods to reduce cooling load were studied such as window-film installations, sun-screens, cabin external colour and cabin ceiling insulation. Hamdan et al. [10] modified a car's air-conditioning vent into a dual direction blower powered by a solar panel placed on the roof of the car. Different cases with conventional temperature control measures and with the modified blower were studied and it was found that the use of the modified blower gave 10° reduction in cabin temperature in comparison to the base case with no air circulation. Similarly, Ciocanea and Buretea [1] developed cross flow fans with two pairs placed under the car roof and under the rear seat shelf with a flow rate of 0.02 m^3/s, which could provide sufficient air flow to reduce the cabin temperatures to a satisfactory level.

Aljubury et al. [11] also carried out experiments with a full-size car parked without shade in six different parking orientations and monitored the cabin temperature at different locations inside the cabin. The air temperature was found to reach a maximum of 70° and dashboard temperature reached 100°. A cardboard shade with windows shut and windows down by 1 cm was also tested. The cardboard shade with closed windows did not reduce air temperature inside the cabin but reduced dashboard temperature by 40%, whereas with windows down by 1 cm, a 70% reduction in temperature inside the cabin was observed.

Vishveshwara and Dhali [12] developed a ventilation system consisting of two fans for removing the hot trapped air in the cabin and supplying ambient air from outside. It was found that the ventilation system almost halved the temperature difference between the cabin air and ambient air. It also reduced the cooling time for the vehicle air-conditioning system after being switched on from a parked state. The system utilized solar power from a PV cell placed on the roof and did not cause any strain on the vehicle battery. Yan et al. [13] have also tested a PV cell powered four axial fan module through CFD simulations for cabin heat removal from a UXV electric vehicle.

Senthilkumar et al. [14] have carried out a numerical analysis of the heat accumulation inside a truck cabin and predicted the hot spots generated due to solar radiation. They have accounted for the various materials used inside an automobile cabin and predicted the thermal hot spots based on solar radiation incident at different angles and intensities. Leong et al. [15] have carried out CFD simulations for the cabin heat removal from an electric car. They have concluded that the solar radiation entering from the windshield and window glass contribute to the maximum heat accumulation inside the cabin and then used a ventilation system with different inlet velocities, identifying an optimal flow rate for effective heat removal from the cabin and reduction of cabin and seat temperatures. Giri et al. [16] have also carried out a similar 2-D analysis of using different inlet velocities.

Several studies [16–20] have been performed on increasing the efficiency and managing the environmental impact of mobile air-conditioning systems. New developments for increasing heat transfer effectiveness for these systems suggest use of phase change materials [21–23]. Studies focusing on the enhancement of solar power output using current technology also provide alternative energy sources to manage the ventilation and air-conditioning systems in a car cabin [24]. Some of the technologies were invented for climate control of parked cars [25–27] with some focusing on use of solar power for automobile air-conditioning systems [28, 29].

CFD simulations have proved useful in the design and evaluation of various heat transfer devices such as gas

coolers, absorption refrigeration systems, heat exchangers, thermosyphons, etc. [30–35]. These studies substantiate the usability of CFD in evaluation of heat transfer effects in a system.

From the literature review, it is found that cabin heat management has been studied either by experimental method or numerical analysis with 1D/2D assumptions. Most of the studies with numerical and experimental techniques have used fixed solar heat flux values or artificially creating the solar thermal irradiation environment with an infrared light source which may not be completely mimicking the solar thermal environment. Up to authors' knowledge, there have not been any studies involving both experimental and numerical techniques with real solar thermal irradiation along with consideration of the orientation of vehicle.

Hence, the present study aims at predicting the transient temperature evolution inside a car cabin placed in a realistic solar thermal conditions through both experimental and numerical techniques and solving the issue of excessive heat removal from car cabins through the use of individual and combinations of conventional cabin cooling methods and suggest the most effective method based on experimental and computational results. Numerical solar calculator model available in ANSYS Fluent [36] is also assessed with the experimental results of the baseline model and then, different methods of cabin heat management such as tinted windows, rolled down windows and a ventilation system with different mass flow rates have been analysed numerically along with combinations of the same to get a better understanding of the phenomenon and determine the most effective and efficient method employable.

Experimental

A 5:1 scale down model of a car cabin is setup for solar load experiment as shown in Fig. 1. The interior of the cabin model consists of a dashboard, two front seats and one rear seat. The four pieces of glass are attached using Silicone adhesive. The wooden parts are nailed and the glass is attached to it using transparent duct tape to ensure proper sealing. Six holes are drilled through the bottom for placement of thermocouples to measure the temperature. The six locations are dashboard, two front seats, two in rear seat and one behind the rear seat in the luggage area as shown in Fig. 2. A temperature sensing meter having six channels is used to read the temperature. PT-100 resistance thermometers, also called resistance temperature detectors (RTDs), have been employed which use Platinum as the sensing material due to its inert nature. The range of PT-100 is from 0 to 100 °C with an accuracy of ± 0.1 °C.

The dimensions are taken as 50 cm (length) × 24.4 cm (width) × 14.4 cm (height) [9]. The front and rear tilted angles are 35° and 45°, respectively. Figure 3 shows the design and dimensions for each component. The material properties are presented in Table 1 for plywood and fibreglass.

The material used for the frame (the dashboard and side panels) of the experimental model is wood. The material selection can be attributed by the facts that the heat transfer between the frame body and the interior is very limited according to the work of Alexandrov et al. [37], and that modern cars have a double layer structure to provide insulation inside the cabin, a similar insulation can be provided through the use of wood in a scaled down model. And also as this study is performed for soaking condition of a vehicle

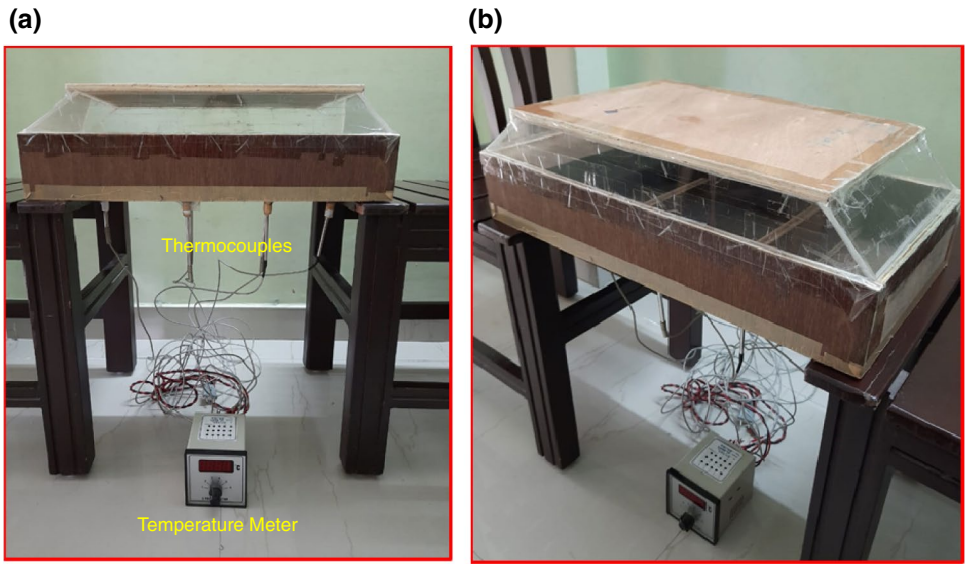

Fig. 1 Physical model used in experiment. **a** Side view. **b** Isometric view

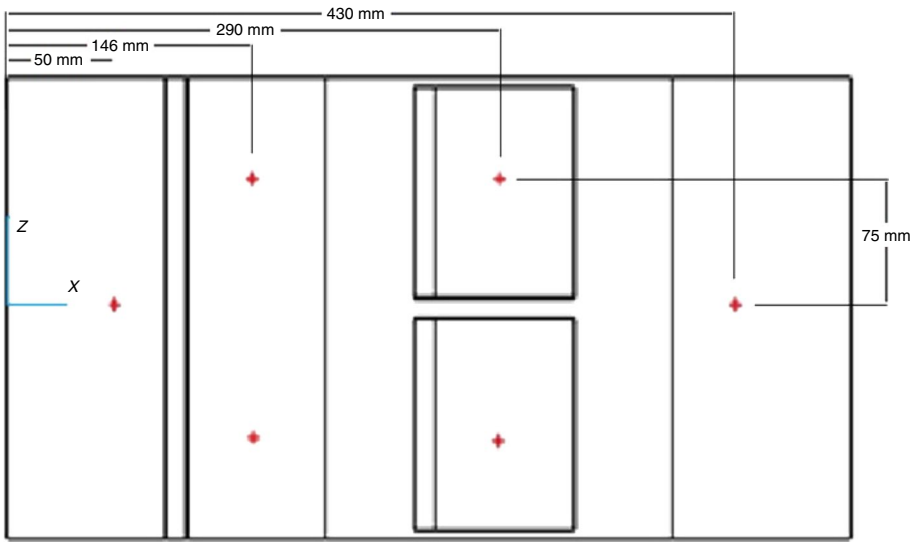

Fig. 2 Locations of PT-100 thermocouples

so heat penetration from engine side is also neglected. The material definition has been kept consistent in the simulations as well. Hence the material selection is justified for realistic condition.

The model has been kept facing South on 20 February 2019 at 10:00 am in the morning. Using the temperature meter, temperature values from all six locations are noted at 1-min intervals.

Numerical modelling

The experiment has been recreated for numerical analysis through ANSYS Fluent where a 3D model of the car cabin has been tested using appropriate boundary conditions [36]. Figure 4 shows different views for the model used with dimensions consistent with the experiment. Figure 5 shows the mesh structure for the model.

Grid independence study-validation

A grid independence study has been performed to establish that the mesh does not influence the accuracy of the results. Several grid densities have been tested as shown in Table 2. It is observed that a grid density of 0.9 million is sufficient to remove the influence of grid and increasing the density further does not change the results.

A pressure-based solver has been used for solving viscous laminar cases with energy equation. The properties of all the materials have been defined and a surface to surface radiation model has been employed. Solar loads have been defined using solar load calculator [36] with Chennai's latitude and longitude. The solar load calculator ensures the similar sun conditions in the computational case as that of the experimental. Hence, the influence of time and date and the corresponding sun conditions have been eliminated in the comparison. The time has been kept consistent with the experiment and clear weather conditions are defined. The temperature observations are made for the same time and date in both experimental and computational cases. The duration of temperature observation used here has been limited to 30 min as the computational time is very expensive. Different numbers of faces per cluster have been tested and finally it has been kept at 10 as shown in Fig. 6. The boundary conditions have been presented in Table 3.

The temperature contours predicted through numerical simulations at different locations inside the cabin show proper consistency with the direct sunlight patterns observed in the experiment as shown in Fig. 7.

Figure 8 shows the comparison of temperatures obtained from both the experimental and numerical methods measured at various locations such dashboard, right front seat, right back seat, left front seat, left back seat and luggage compartment. It can be noticed that the dashboard has the highest temperature and the left back seat has the lowest temperature among all the sides at the end of testing duration. This could be attributed by the fact the solar irradiation can easily transmitted through windshield and windows, and however, in this case as the vehicle is oriented towards south, transmission of radiation is less on the left-side seats due to shadowing effect which can be clearly seen from both the experimental and numerical temperature contours in Fig. 7. And also the window glasses are fixed vertically as compared with dashboard and luggage compartment glasses which are inclined with some angles. Because of these reasons, temperature increment due to solar transmitted radiation contribution is more in the dashboard, luggage compartment sides as compared to that in the right-hand side windows which is evident from Fig. 7. The temperature values for the left hand front and back seats are lower than those of right-hand side seats because of the orientation effect.

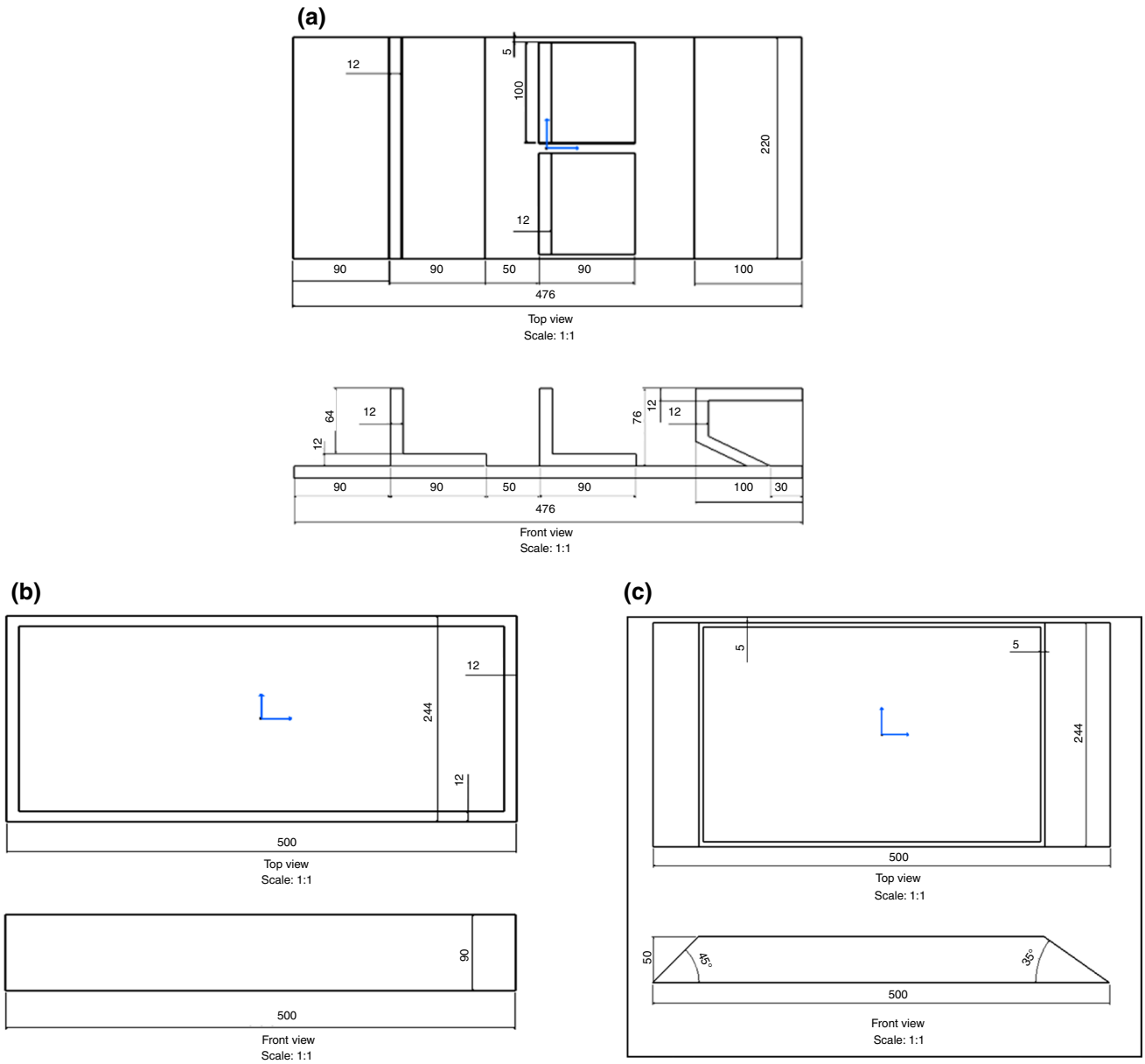

Fig. 3 Cabin dimensions in mm. **a** Interior. **b** Walls. **c** Windshield and windows

Table 1 Properties of materials

Property	Plywood	Fibreglass
Density/kg m^{-3}	900	2800
Specific heat capacity/J kg^{-1} K	1215	840
Thermal conductivity/W m^{-1} K	0.12	0.8
Emissivity	0.8	0.8
Absorptivity	0.8	0.2
Transmissivity	0	0.5
Reflectivity	0	0.1

The average percentage deviation is calculated by comparing the temperature values at each time interval from both the experimental and numerical results. The average percentage deviations are 10.57%, 3.10%, 1.96%, 1.98%, 3.62%, 9.88% for the dashboard, right front seat, right back seat, left front seat, left back seat, luggage compartment locations, respectively. It can be noticed that the maximum average percentage deviation is 10.57% in the dashboard readings and the minimum average percentage deviation is 1.96% in the right front seat readings. These deviations may be due the numerical accuracy of the solar model available in ANSYS

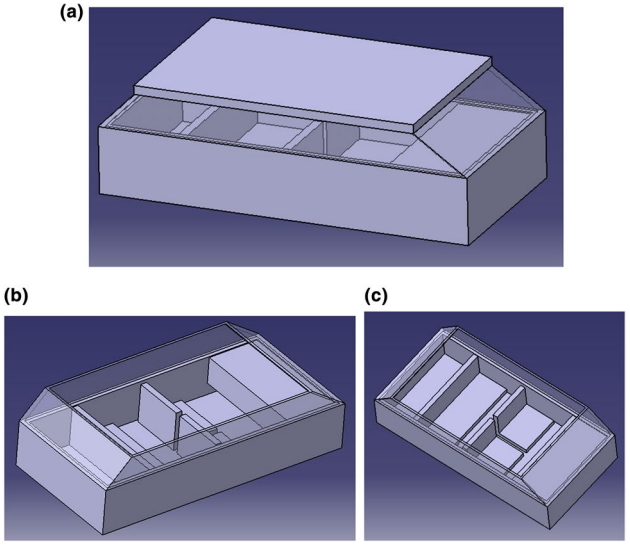

Fig. 4 Cabin assembly views

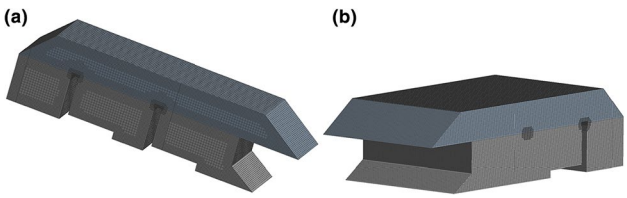

Fig. 5 Mesh structure. **a** Sliced mesh. **b** Full domain mesh

Table 2 Grid independence study

Mesh size	Dashboard temperature /°C	Left front/ back seat /°C	Right front/ back seat /°C	Luggage temperature /°C
6 lakhs	15	12	14	15
9 lakhs	32	30	31	31
12 lakhs	32	30	31	31
15 lakhs	32	30	31	31

Fluent which uses a clear weather condition in which all the local environmental effects cannot be considered.

Results and discussion

Further analyses have been carried out using a similar grid structure as used for validation. Different cabin temperature reduction techniques have been tested individually and in combination to obtain the best possible case for effect cabin temperature control.

Use of new tint technology (TYPE 1)

Electrochromic tinting technology uses a small potential difference supplied across a material causing a redox reaction which changes the colour or opacity of the material. Energy supply is only required to cause a change and the changed colour or opacity is persistent, enabling the user to determine the amount of heat and light allowed to pass. Using this for a car windshield, the amount of heat entering the car through the windshield can be greatly reduced by making it opaque when the car is parked.

In the numerical model, only the front windshield is considered to be of electrochromic material. Side window panels and rear windshield are considered to be having tint films as per regulations. The visible light transmission (VLT) for front windshield is taken to be 10%, for rear windshield 75% and for the side window panels it is taken as 50%. So, the transmissivity value of fiberglass has been changed accordingly at these locations. Figure 9 shows the difference in temperature for baseline model vs the model with above-mentioned tints. The plots for left front and back seats are found to be identical. The right front and back seats also follow the same pattern.

A significant 13 °C reduction in dashboard temperature is observed in this case as the primary source of heat for the dashboard is the front windshield. However, the other cabin locations see minor temperature reductions with 1 °C reduction for left front and back seats and 3 °C reduction for right front and back seat. The luggage compartment temperature reduced by 5 °C. This signification reduction in dashboard temperature may be due to the fact that front windshield allows less solar radiation as its transmissivity is 0.1, while right-hand side seats (transmissivity is 0.25) and luggage compartment (transmissivity is 0.35) allow more radiation to the cabin. Minor temperature reduction in left hand side seats can be justified by the fact that solar radiation transmission is very less due to the vehicle orientation effect and that the influence of tint glass is also minimal in temperature reduction.

Use of inlet and outlet vents (TYPE 2)

Inlet and outlet vents can be employed to refresh the air inside a parked car cabin removing the hot accumulated air. For the present case, inlet vents (diameter 10 mm) are positioned near the rear seat and floor region and outlet vents (diameter 15 mm) are present on the car dashboard as shown in Fig. 10. The vents are powered by the car battery which can be recharged using solar panels positioned on the roof. The inlet blower volume flow rates are taken as 30 cfm, 60

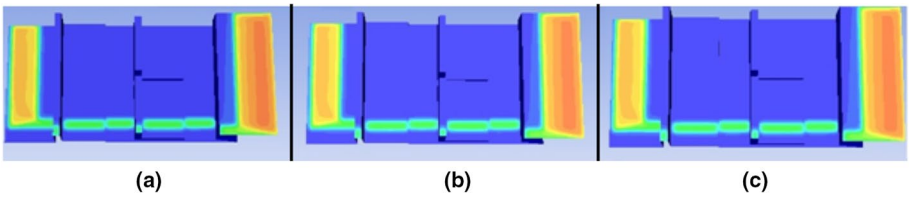

Fig. 6 Faces per surface cluster. **a** 1. **b** 10. **c** 100

cfm and 100 cfm and the corresponding outlet mass flow rates are calculated as 0.016 kg/s, 0.033 kg/s and 0.055 kg/s, respectively. Figure 11 shows the plots for temperature variation inside the cabin for all three mentioned mass flow rates compared with the baseline case.

It is observed that low mass flow rate gives 6 °C reduction for dashboard temperature, whereas medium and high mass flow rates gave 7 °C reduction. The left- and right-side seats undergo 1 °C and 3 °C reduction, respectively, for all mass flow rates. The luggage compartment temperature reduced in 1 °C steps from 3 °C to 5 °C for low to high mass flow rates. Hence, increasing the mass flow rate is observed to give better reduction in cabin temperatures. The effect is more significant at dashboard side since in the present study, the outlet vents are located on the dashboard which help to bring more air flow in that region as compared to other locations. However, effect of inlet and outlet vent locations can be studied further by modifying these locations in the future work.

Table 3 Boundary conditions

Physics	Boundary conditions	Types/values	
		wood (frame)	Glass (windshield, windows)
Momentum	Wall motion	Stationary wall	Stationary wall
	Shear condition	No slip	No slip
Thermal (mixed condition)	Material	Plywood	Fibreglass
	Heat transfer coefficient	10	10
	Free Stream Temperature	303	303
	External emissivity	0.8	0.8
	Internal emissivity	0.8	0.8
	Wall thickness	12 mm	5 mm
	Shell conduction	ON	ON
Radiation	BC Type	Opaque	Semi-transparent
	Participates in solar ray tracing	ON	ON
	Absorptivity	0.8	0.2
	Transmissivity	0.0	0.5
	Faces per cluster	10	10
	Participates in view factor calculation	ON	ON

Using tints with inlet and outlet vents (TYPE 3)

The previous two cases are then combined to observe the effect on cabin temperatures. The VLT for all glasses and the vent locations and diameters are same as the previous cases. A mass flow rate of 0.033 kg/s is selected for the vents as it gives better cooling than 0.016 kg/s and comparable cooling to 0.055 kg/s. Figure 12 shows the plots for this case compared with the baseline case.

In this case, a 14 °C reduction is observed at the dashboard, 1 °C at left-side seats, 4 °C at right-side seats and 6 °C reduction is seen in the luggage compartment. The combination of the two methods gave best temperature reduction for the dashboard. The trend in temperature reduction in this case is almost the same as they appear in the TYPE 1 and TYPE 2 cases. However, the benefits from this combined technique are not directly equal to the summation of benefits achieved by those two individual techniques. So, a trade-off concept can be followed when it comes to real-time applications based on the power requirement for achieving air flows through inlet and outlet vents.

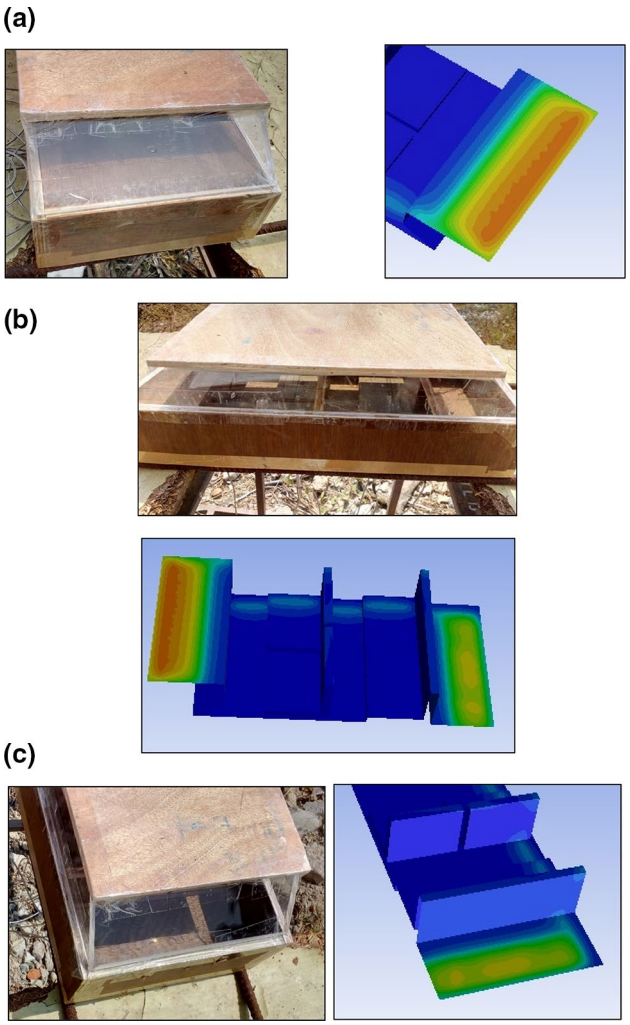

Fig. 7 Comparison of temperature contours from numerical analysis with experiment. **a** Dashboard. **b** Side view with dashboard on left and luggage compartment on right. **c** Luggage compartment

Using tints with outlet vents and lowered windows (TYPE 4)

Further a new case is tested where the inlet vents are replaced by lowered windows. The windows are lowered by 2 mm and the outlet vents are again positioned as before at the dashboard. Tints are present as in the previous case, and a mass flow rate of 0.033 kg/s is selected again. Figure 13 shows the plots for temperature variation inside the cabin compared with the baseline.

Here again a 14 °C reduction is observed at the dashboard, 1 °C and 5 °C reductions for left- and right-side seats, respectively, and 6 °C reduction for the luggage compartment. This case is comparable in effectiveness to the previous and better reduction is observed only in the right-side seat temperatures. The reason for this marginal improvement when combined with tint case (TYPE 1) could be attributed by the flow of air coming in through open windows instead of inlet vents. However, keeping the windows open is not advisable for safety aspects even though the gap is only 2 mm.

Comparison of different systems

One baseline and four different cooling configurations have been studied in the present study. A comparison of temperature plots for all these cases is presented in Fig. 14. It is observed that the use of tints in any case gives a very good reduction in dashboard temperatures. Further vents and lowered windows give mostly comparable results although lowering windows gives better results for seat temperatures. Combined cooling methods are the most useful and can give good control of cabin temperatures in real-life applications.

Cooling load calculations

The heat loads for the baseline and for the different heat removal systems are calculated using one dimensional heat transfer approach including conduction, convection and radiation modes through the thermal resistance concept. The total heat load accumulation inside the car cabin is calculated by adding the heat transfer through both wood and glass materials and can be expressed as follows:

$$Q = Q_{\mathrm{w}} + Q_{\mathrm{g}}(\mathrm{W}) \tag{1}$$

where, Q_{w} denotes the rate of heat transfer through opaque material (i.e. plywood) and Q_{g} stands for the rate of heat transfer through transparent material (i.e. fiberglass).

In heat transfer calculation for the opaque material, both the conduction and convection heat transfers are considered and the radiation is neglected as the transmissivity is zero. The rate of heat transfer (Q_{w} can be expressed as follows:

$$Q_{\mathrm{w}} = U_{\mathrm{w}} \times \Delta T \times A(\mathrm{W}) \tag{2}$$

where, A is the total surface area of opaque material which is equal to 0.1968 m^2, and ΔT is the difference between the outer cabin surface temperature and the average cabin inside temperature.

The overall heat transfer coefficient (U_{w}) due to opaque material is given by

$$U_{\mathrm{w}} = \frac{1}{\frac{1}{h_{\mathrm{i}}} + \frac{t}{k} \times n}\left(\mathrm{Wm}^{-2}\,\mathrm{K}^{-1}\right) \tag{3}$$

where, h_{i} is the internal heat transfer coefficient, t is the thickness, n is the number of surfaces (=4) and k is the thermal conductivity of wood. It is to be noted that the outside heat transfer coefficient is assumed to be negligible as the

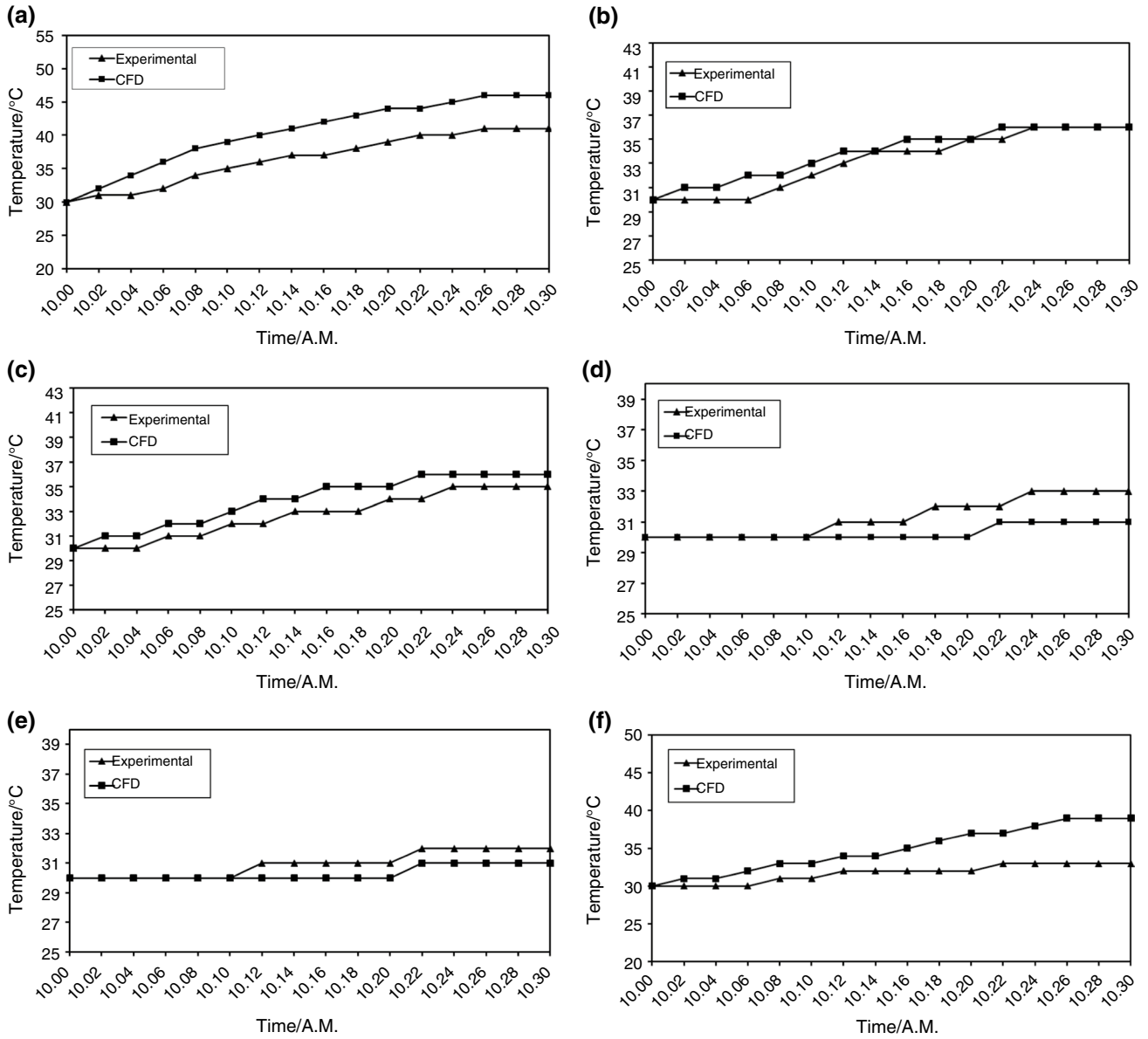

Fig. 8 Comparison of temperature with time for experimental and CFD results at. **a** Dashboard. **b** Right front seat. **c** Right back seat. **d** Left front seat. **e** Left back seat. **f** Luggage compartment

variation of outside temperature is not significant during the 30 min time period. Hence, Eq. (2) gives the heat penetration through the opaque material (Q_w) as 3.73 W.

In heat transfer calculation for the transparent material, all the heat transfer modes, namely conduction, convection and radiation are considered. Hence the heat transfer through transparent material (Q_g) can be expressed as follows:

$$Q_g = U_g \times A_g \times \Delta T + (\text{Diffused radiation})_{CFD} \times A_g \times \tau + (\text{Direct radiation})_{CFD} \times \cos(i) \times A_g \times \tau \quad (4)$$

where U_g is the heat transfer coefficient for glass and calculated using the same procedure used for U_w with respect to the glass wall thickness and thermal conductivity values, A_g is the area of glass, i is the incident angle, τ is the transmissivity value of glass which is considered as 0.5 for the baseline case and for the other cases with tint technology, the values taken as 0.1, 0.25, 0.35 for front windshield, windows, rear windshield, respectively. The diffused and direct solar radiation values are 116.86 W m^{-2} and 1022.5 W m^{-2}, taken from CFD results which are calculated based on the location, date and time conditions specified in the solar calculator.

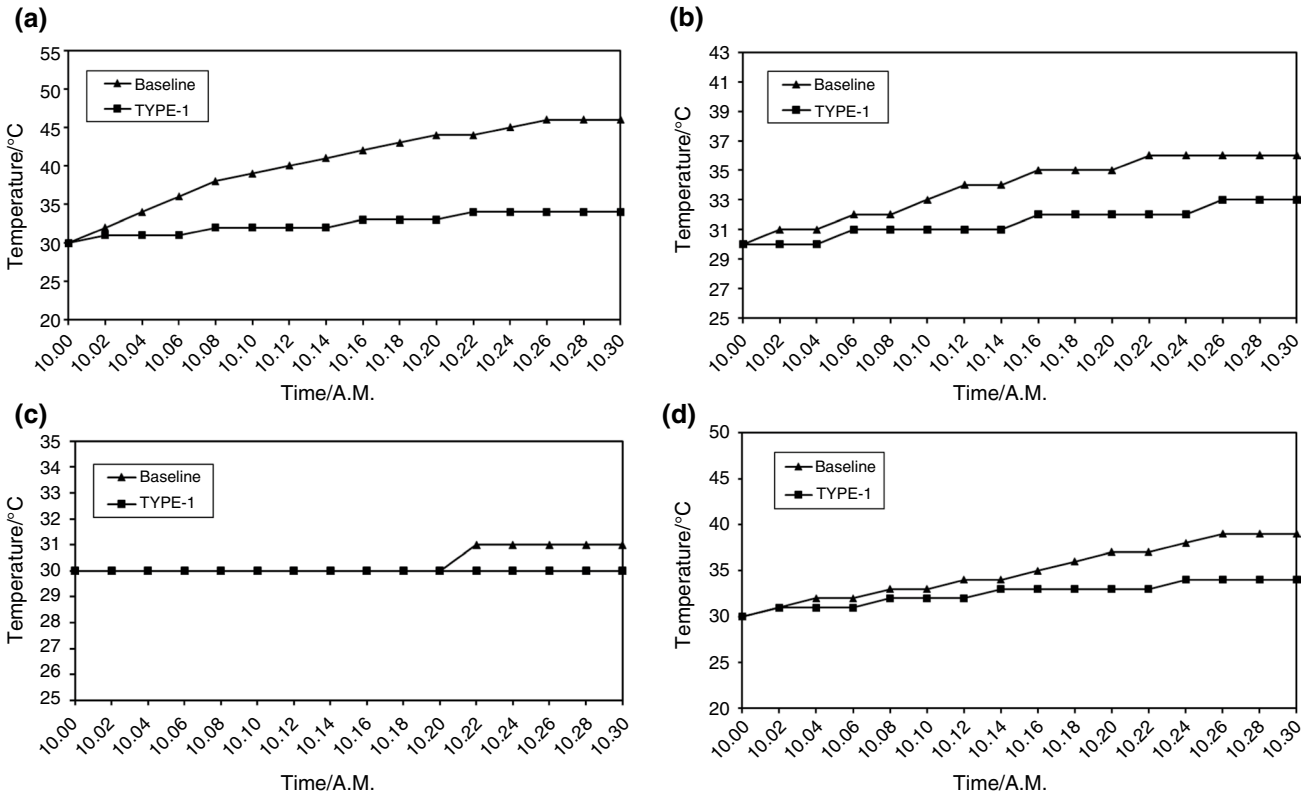

Fig. 9 Comparison of temperature with time for baseline case and TYPE 1 case at. **a** Dashboard. **b** Right-side seats. **c** Left-side seats. **d** Luggage compartment

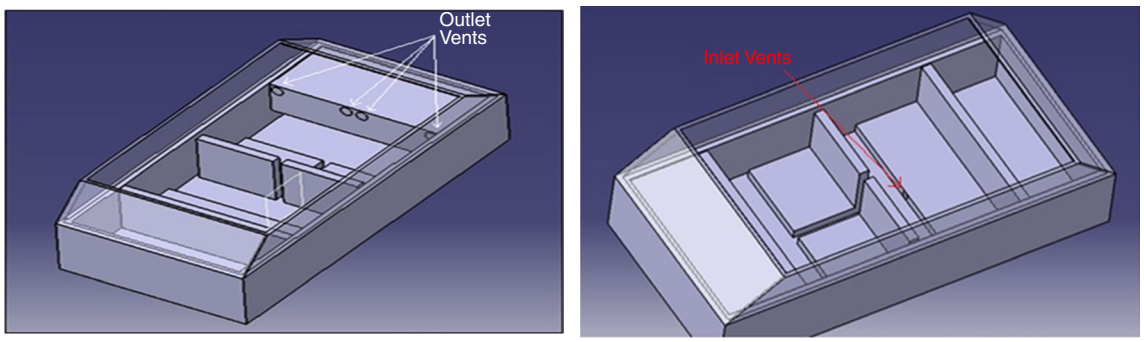

Fig. 10 Location of inlet and outlet vents

Eq (4) gives the heat penetration through the glass (Q_g) as 21.94W for the baseline case. The total heat load (Q) for the baseline can then be calculated based on Eq. (1) and which is equal to 25.67 W. The similar procedure is followed for calculating the total heat loads for other cases also are presented in Table 4.

Table 4 shows also heat load reductions and percentage of reduction for different techniques used as compared with the baseline. It is well known that use of air conditioner causes a significant increase in fuel consumption in real-life scenarios. At full speed an AC unit consumes 3 kW power reducing the fuel economy by 24% [29]. For a stationary car this load amounts to 1.26 kW. With application of the suggested cooling techniques, this load can be reduced by 61.9%

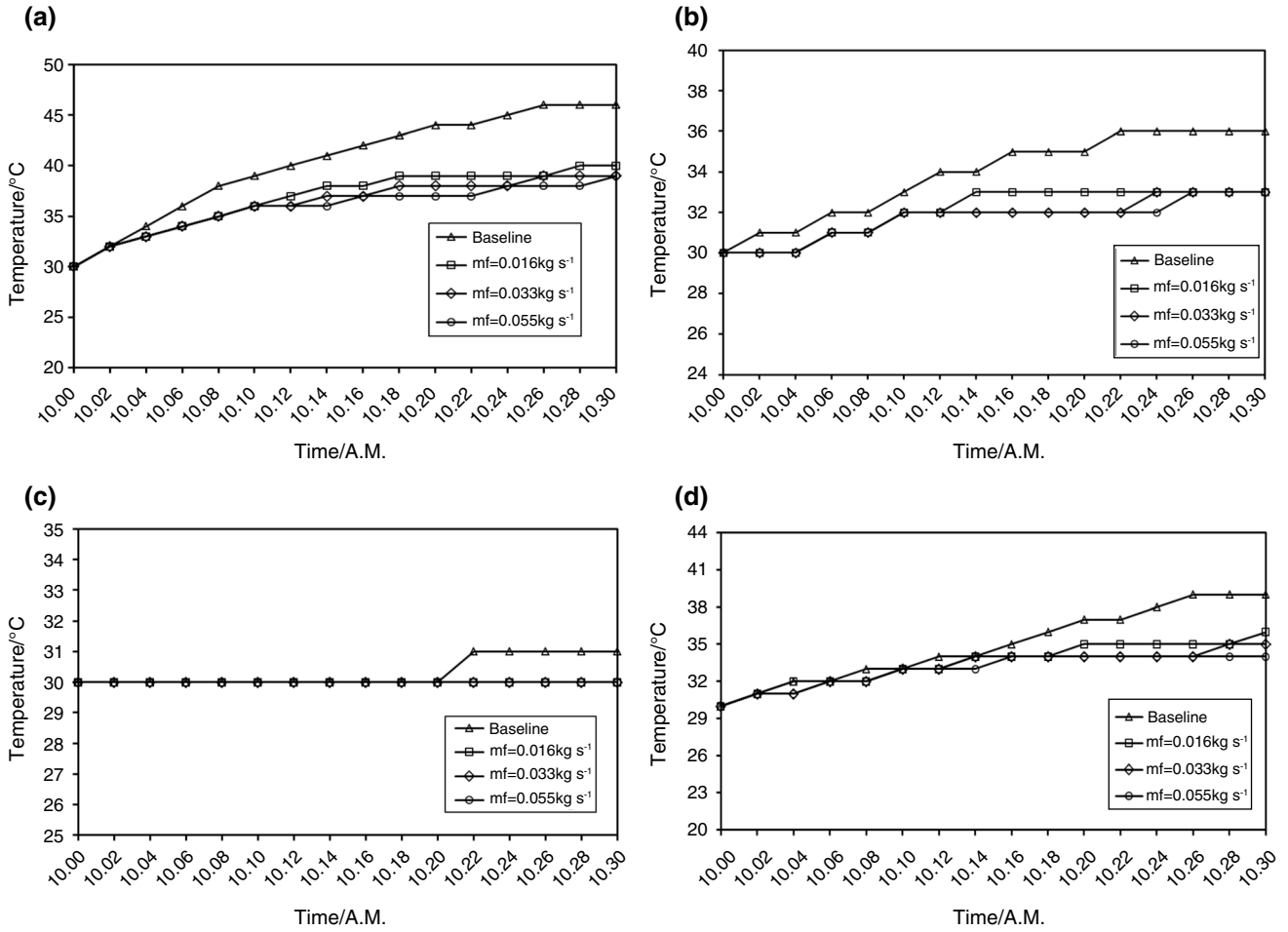

Fig. 11 Comparison of temperature with time for baseline case and TYPE 2 case at. **a** Dashboard. **b** Right-side seats. **c** Left-side seats. **d** Luggage compartment

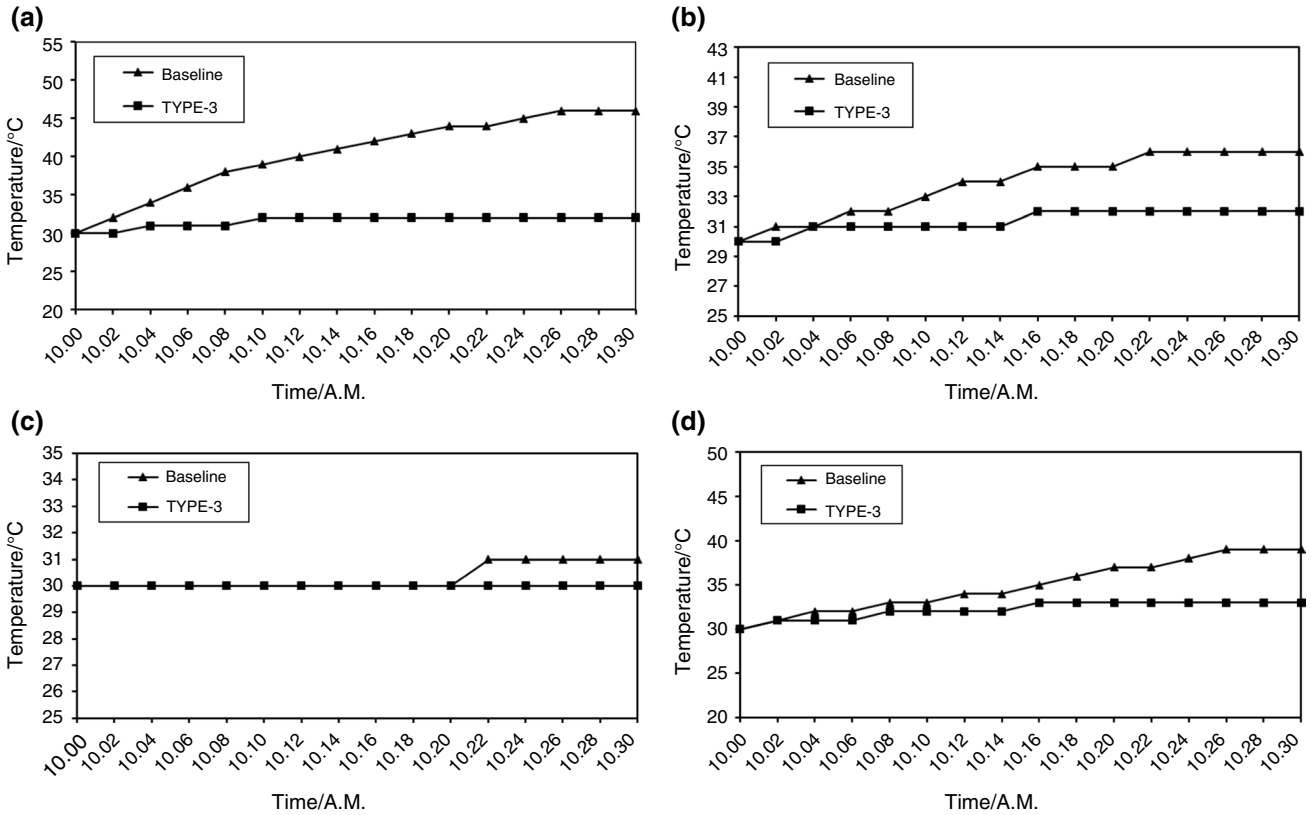

Fig. 12 Comparison of temperature with time for baseline case and TYPE 3 case at. **a** Dashboard. **b** Right side seats. **c** Left-side seats. **d** Luggage compartment

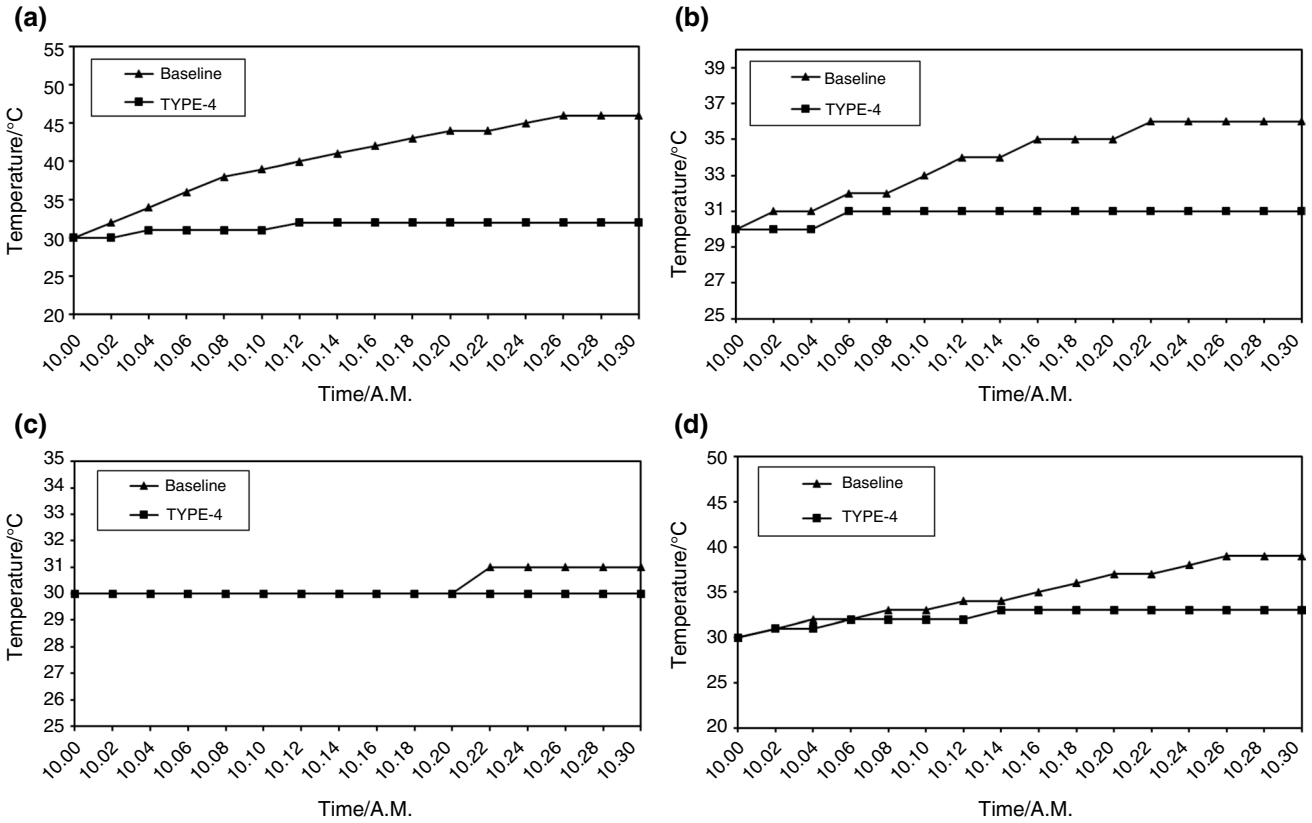

Fig. 13 Comparison of temperature with time for baseline case and TYPE 4 case at. **a** Dashboard. **b** Right side seats. **c** Left-side seats. **d** Luggage compartment

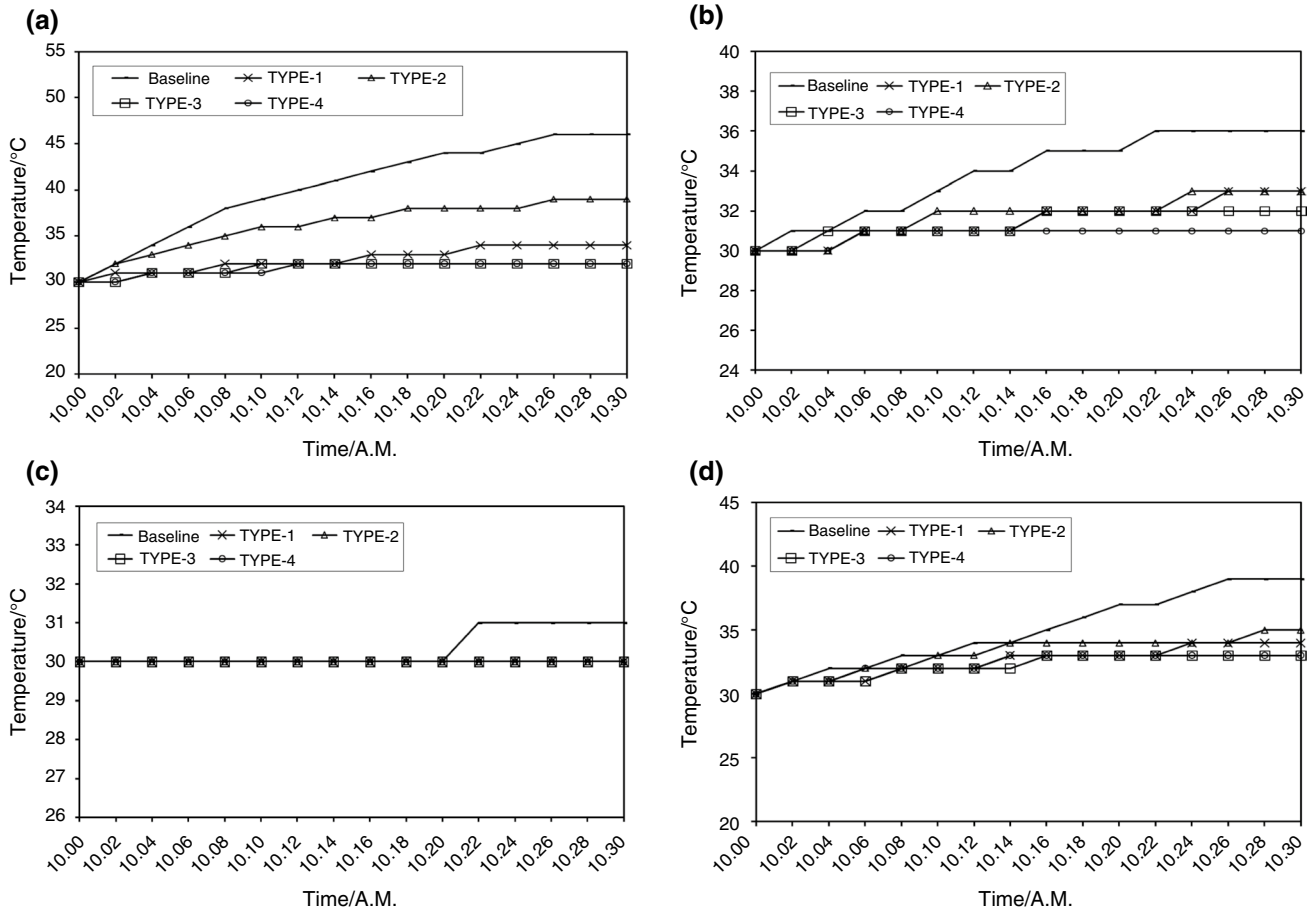

Fig. 14 Comparison of temperature with time for baseline case with all other cases at. **a** Dashboard. **b** Right side seats. **c** Left-side seats. **d** Luggage compartment

Table 4 The percentage of cooling load reduction for various heat removal systems

Case	Average surface temperature *T*s(avg)/°C	Average cabin temperature *T*cabin(avg) /°C	Temperature difference Δ*T*/ °C	Cooling load	Reduction from baseline	% reduction
Baseline	30.0	39.50	9.5	25.67 W	–	–
TYPE 1		34.25	4.25	11.93 W	13.74 W	53.5
TYPE 2		34.75	4.75	21.12 W	4.55 W	17.7
TYPE 3		32.0	2.0	9.77 W	15.9 W	61.9
TYPE 4		32.0	2.0	9.77 W	15.9 W	61.9

to 0.48 kW. This reduced load on engine improves mileage by 6.9% from 16.18 kmpl to 17.3 kmpl.

Conclusions

In the present study, numerical analyses have been performed to suggest an effective technique for control of cabin temperatures of a car parked in direct sunlight. Validation has been performed through an experimental model which validates the baseline analysis. A 5:1 scale model of a car cabin has been tested in direct sunlight placed facing South on 20 February 2019 in Chennai at 10:00 am. Similar conditions have been recreated in the baseline analysis using solar load calculator. The model is subjected to sunlight for a period of 30 min, and the temperature plots at different cabin locations are plotted. The deviation between the numerical and experiments results could be attributed to the

accuracy of the clear weather condition solar model available in ANSYS Fluent.

Different cooling techniques have then been proposed to control the cabin temperatures for a parked car in given conditions, such as use of electrochromic tint on windshield, inlet and outlet vents for air circulation and combinations of these with windows lowered. It is observed that a combination of the techniques provided better temperature reductions with minimal energy requirement. The front windshield is observed to be the major contributor in heating of the cabin, hence, tinting the windshield gives significant reduction in dashboard temperature of 13 °C. Circulation of air inside the cabin through ventilation ensures that the hot air inside the cabin is removed further reducing the temperature of the cabin. Three different mass flow rates for the ventilation system have been tested. Lowered windows also give comparable results as that with inlet vents with lower energy consumption, both giving a maximum reduction of 14 °C.

The comfort level inside a car cabin is thus, greatly influenced by the temperature of the cabin. Use of air conditioner to regulate cabin temperature from a parked state posessess huge stress on the engine and consumes more fuel. Based on the 1-D thermal resistance concept, it is found that cabin temperature control through the proposed techniques can greatly reduce the cooling load on the engine and ensure better fuel economy with 61.9% reduction in cooling load and 6.9% improvement in fuel economy. However, the final selection among these techniques could be made with consideration of safety regulations.

Finally, it has been found that the orientation of the vehicle, the transmissivity of the windows and windshield materials, and the augmented air circulation through vents have huge impact on the cooling load reduction of the vehicle. Hence, further analysis can be performed with a variety of these parameters and can be extended to other vehicles' heat load prediction due to solar radiation by changing geometrical parameters under different tropical conditions.

References

1. Ciocanea A, Laurenţiu BD. Cabin heat removal from parked cars. Mag Hydraul Pneum Tribol Ecol Sens Mechatron. 2014;3:52–8.
2. Booth JN, Davis GG, Waterbor J, McGwin G. Hyperthermia deaths among children in parked vehicles: an analysis of 231 fatalities in the United States, 1999–2007. Forensic Sci Med Pathol. 2010;6(2):99–105.
3. Johnson VH. Fuel used for vehicle air conditioning: a state-by-state thermal comfort-based approach. SAE Tech Pap. 2002; 2002-01-1957.
4. Sen S, Selokar M. Numerical simulation and validation of cabin aiming and cool-down of a passenger car. SAE Int J Passeng Cars Mech Syst. 2016;9(1):52–61.
5. Khatoon S, Kim M. Human thermal comfort and heat removal efficiency for ventilation variants in passenger cars. Energies. 2017;10(11):1710.
6. Jha KK, Bhanot V, Ryali V. A simple model for calculating vehicle thermal loads. SAE Tech Pap. 2013; 2013-01-0855.
7. Patil A, Radle M, Shome B, Ramachandran S. One-dimensional solar heat load simulation model for a parked car. SAE Tech Pap. 2015;2015-01-0356.
8. Arya G. Cabin temperature control of a parked car through forced ventilation. M.E. Thesis, Thapar University, India; 2015
9. Tseng C-Y, Yan Y-A, Leong JC. Thermal accumulation in a general car cabin model. J Fluid Flow, Heat Mass Transf. 2014;1:48–56.
10. Hamdan NS, Radzi MFM, Damanhuri AAM, Mokhtar SN. Dual direction blower system powered by solar energy to reduce car cabin temperature in open parking condition. J Phys Conf Ser. 2017;908(1):012072.
11. Mohammed I, Aljubury A, Farhan AA, Mussa A. Experimental study of interior temperature distribution inside parked automobile cabin. J Eng. 2015;21(3):1–10.
12. Vishweshwara SC, Dhali JMA. Experimental investigations on the performance of solar powered cabin air ventilator. World J Eng. 2015;12(6):607–18.
13. Yan Y, Tseng C, Leong JC. Feasibility of solar powered cooling device for electric car. Energy Procedia. 2012;14:887–92.
14. Senthilkumar S, Ramkumar K, Velshankar M, Karthikeyan S, Parthipan D. Numerical modeling of solar radiation heat transfer for a truck cabin. Appl Mech Mater. 2015;813–814:742–7.
15. Leong JC, Tseng C-Y, Tsai B-D, Hsiao Y-F. Cabin heat removal from an electric car. World Electr Veh J. 2010;4(4):760–6.
16. Giri A, Tripathi B, Thakur HC. 2-D CFD analysis of passenger compartment for thermal comfort and ventilation. Int J Eng Manuf Sci. 2017;7(1):38–42.
17. Prabakaran R, Lal DM, Devotta S. Effect of thermostatic expansion valve tuning on the performance enhancement and environmental impact of a mobile air conditioning system. J Therm Anal Calorim. 2020. https://doi.org/10.1007/s10973-019-09224-2.
18. Prabakaran R, Mohan Lal D. A novel exergy based charge optimisation for a mobile air conditioning system: an experimental study. J Therm Anal Calorim. 2018;132(2):1241–52.
19. Andrew Pon Abraham JD, Mohanraj M. Thermodynamic performance of automobile air conditioners working with R430A as a drop-in substitute to R134a. J Therm Anal Calorim. 2019;136(5):2071–86.
20. Sharif MZ, Azmi WH, Redhwan AAM, Mamat R, Najafi G. Energy saving in automotive air conditioning system performance using SiO 2/PAG nanolubricants. J Therm Anal Calorim. 2019;135(2):1285–97.
21. Moazzez AF, Najafi G, Ghobadian B, Hoseini SS. Numerical simulation and experimental investigation of air cooling system using thermoelectric cooling system. J Therm Anal Calorim. 2019. https://doi.org/10.1007/s10973-019-08899-x.
22. Omara AAM, Abuelnuor AAA, Mohammed HA, Khiadani M. Phase change materials (PCMs) for improving solar still productivity: a review. J Therm Anal Calorim. 2019. https://doi.org/10.1007/s10973-019-08645-3.
23. Antony FRM, Joseph SS. Investigation of energy and exergy performance on a small-scale refrigeration system with PCMs inserted between coil and wall of the evaporator cabin. J Therm Anal Calorim. 2019;136(1):355–65.
24. Sakhaei SA, Valipour MS. Investigation on the effect of different coated absorber plates on the thermal efficiency of the flat-plate solar collector. J Therm Anal Calorim. 2019. https://doi.org/10.1007/s10973-019-09148-x.
25. Futernik V, Futernik B. Temperature control system in a parked vehicle. 2013. Patent No. US 8468843 B2.
26. Galvez-Ramos AM. Climate control system for parked automobiles. 2009. Patent No. US 2009/0130965 A1.

27. Galvez-Ramos AM. Air cooling system for parked automobiles. 2007. Patent No. US 2007/0245755 A1.
28. Costanzo PE, Wremham. Solar powered chilled cooler. 2007. Patent No. US 2007/0240442 A1.
29. Qiang C, Chao S, Zhongchao W. Solar air conditioner and power supply method of same. 2013. Patent No. CN 103208837 A.
30. Santosa IdMC, Tsamos KM, Gowreesunker BL, Tassou SA. Experimental and CFD investigation of overall heat transfer coefficient of finned tube CO2 gas coolers. Energy Procedia. 2019;161:300–8.
31. Lima AAS, Ochoa AAV, Da Costa JAP, Henríquez JR. CFD simulation of heat and mass transfer in an absorber that uses the pair ammonia/water as a working fluid. Int J Refrig. 2019;98:514–25.
32. Abushammala O, Hreiz R, Lemaître C, Favre É. Optimal design of helical heat/mass exchangers under laminar flow: CFD investigation and correlations for maximal transfer efficiency and process intensification performances. Int J Heat Mass Transf. 2020;153:119610. https://doi.org/10.1016/j.ijheatmasstransfer.2020.119610.
33. Wan Y, Soh A, Shao Y, Cui X, Tang Y, Chua KJ. Numerical study and correlations for heat and mass transfer coefficients in indirect evaporative coolers with condensation based on orthogonal test and CFD approach. Int J Heat Mass Transf. 2020;153:119580. https://doi.org/10.1016/j.ijheatmasstransfer.2020.119580.
34. Tabase RK, Van linden V, Bagci O, De Paepe M, Aarnink AJA, Demeyer P. CFD simulation of airflows and ammonia emissions in a pig compartment with underfloor air distribution system: model validation at different ventilation rates. Comput Electron Agric. 2020;171:105297. https://doi.org/10.1016/j.compag.2020.105297.
35. Wang X, Liu H, Wang Y, Zhu Y. CFD simulation of dynamic heat transfer behaviors in super-long thermosyphons for shallow geothermal application. Appl Therm Eng. 2020;174:115295. https://doi.org/10.1016/j.applthermaleng.2020.115295.
36. ANSYS Fluent 14.2 Tutorial Guide.
37. Alexandrov A, Kudriavtsev V, Reggio M. Analysis of flow patterns and heat transfer in generic passenger car mini-environment. In: 9th annual conf of the CFD society of Canada; 2001:27–29.

Publisher's Note Springer Nature remains neutral with regard to jurisdictional claims in published maps and institutional affiliations.